Catalysis Today 143 (2009) 17–24

Contents lists available at ScienceDirect

Catalysis Today

journal homepage: www.elsevier.com/locate/cattod

The steam reforming of phenol over natural calcite materials

Domna A. Constantinou, Angelos M. Efstathiou *

Heterogeneous Catalysis Laboratory, Department of Chemistry, University of Cyprus, P.O. Box 20537, CY 1678 Nicosia, Cyprus

A R T I C L E   I N F O

Article history:
Available online 9 December 2008

Keywords:
Phenol steam reforming
Hydrogen production
Natural calcites
CO_2-TPD
CO_2-DRIFTS

A B S T R A C T

Five natural calcite materials of different geographical origin were studied towards the steam reforming of phenol reaction and the activity results obtained were correlated with some of their physico-chemical properties. It was found that the specific catalytic activity (μmol/(m^2 s)) of the calcite material following calcination at 850 °C was not correlated with the BET area and the primary crystal size of calcium oxide (CaO). The metal impurity levels of the natural calcite materials investigated were found to be very low as evidenced by EDX and XPS measurements, leading to the conclusion that their effect on the catalytic chemistry of phenol steam reforming and surface adsorption properties of CaO was minor. These results suggest that the reaction at hand depends on the heterogeneity and site reactivity present in each CaO surface examined. On the other hand, based on diffuse reflectance infrared Fourier transform spectroscopy (DRIFTS) CO_2 chemisorption and TPD-CO_2 mass spectrometry studies, it was found that the catalytic activity can be correlated with the amount of CO_2 adsorbed at 25 °C in the unidentate form. The latter species was found to be significantly more thermally stable than the bicarbonate adsorbed species also populated on the CaO surface after CO_2 chemisorption (15 Torr) at 25 °C. The least concentration of unidentate carbonate species accumulated on the catalyst surface the higher the catalytic activity of CaO to be expected. It was found that the presence of hydrogen in the feed stream results in a significant decrease of steam reforming of phenol activity over CaO. This result was probed to be likely related to the reduction in the rate of water dissociation to form –OH species, as revealed by the significant decrease in the concentration of adsorbed bicarbonate and –OH species on the surface of CaO according to *in situ* DRIFTS-CO_2 adsorption experiments in the presence of water and of varying hydrogen concentration in the feed. The inhibiting role of H_2 during steam reforming of phenol over CaO is discussed.

1. Introduction

Hydrogen is receiving considerable attention as an important energy carrier as well as a clean fuel for transportation, especially for fuel cell applications [1,2]. The catalytic steam gasification of biomass could be considered as a promising technology for the production of hydrogen-rich gas streams resulting to limited CO_2 and other greenhouse gas emissions. However, one of the important issues associated with the practical application of biomass gasification is the elimination of tars, which leads to clogging of fuel lines and blockage of filters and heat exchangers [3]. The addition of steam was found to produce a lower amount of refractory tars and to enhance the formation of phenol that can be easier reformed catalytically. Therefore, phenol appears to be one of the main constituent molecules of tar composition, in particular when wood-biomass is used in the gasification process [4–6].

A limited number of research works were reported in the literature [7–10] regarding the steam reforming of phenol towards hydrogen production. Supported nickel catalysts are in general the widely used industrial catalysts for gasification/reforming reactions of aromatics [7] for fixed-bed catalytic reactor applications. However, the ability of using appropriate natural materials should be considered very efficient in fluidized-bed reactor applications because of the non-negligible loss of material occurred. Calcined dolomites ($CaMg(CO_3)_2$) and olivines ($(Mg,Fe)_2SiO_4$) are the most investigated natural materials for tar conversion in biomass gasification processes, whereas calcite materials ($CaCO_3$) are the least investigated ones [11–13]. These naturally occurring materials are inexpensive, non-toxic, and abundant with good activity at high temperatures [11].

The use of natural calcites appears as an interesting innovative class of catalytic materials for enhancing the hydrogen yield in conventional biomass steam gasification processes. The calcium oxide (CaO)-containing natural materials can act both as catalysts and as absorbents of CO_2, thus combining the reforming, water–gas shift, and the CO_2 adsorption individual reaction steps into a single

---

* Corresponding author. Tel.: +357 22 892776; fax: +357 22 892801.
E-mail address: efstath@ucy.ac.cy (A.M. Efstathiou).

0920-5861/$ – see front matter © 2008 Elsevier B.V. All rights reserved.
doi:10.1016/j.cattod.2008.10.032

step [6,14–16]. In particular, a comparison of the CO_2 absorption capacity over various calcite, dolomite and olivine natural materials in the 600–850 °C range under absorption-enhanced reforming (AER) conditions [6] led to the conclusion that, in general, calcite natural materials (after calcination at 850 °C) present better CO_2 chemisorption properties than dolomite and olivine.

The main objective of the present work was the study of the steam reforming of phenol reaction towards hydrogen production in a fixed-bed micro-reactor over a series of natural calcite materials of different geographical origin [6], whereas *for the first time* correlations between the specific catalytic activities observed and the main physico-chemical properties of the calcite materials investigated were attempted. For this purpose, BET, X-ray diffraction (XRD), energy dispersive X-ray (EDX) chemical analysis, CO_2 temperature-programmed desorption (TPD), and *in situ* diffuse reflectance infrared Fourier transform spectroscopy (DRIFTS) CO_2 chemisorption and desorption studies were conducted.

2. Experimental

2.1. Catalysts characterization

2.1.1. BET surface area and X-ray diffraction studies

The natural calcite materials were characterized by the BET method (adsorption of N_2 at 77 K) using a Micromeritics Gemini III Surface Area and Pore size Analyser. The specific surface area (m^2/g) of calcites was measured after *ex situ* calcination in ambient air at 850 °C for 2 h followed by *in situ* thermal treatment in N_2 gas at 200 °C for 4 h. The primary mean crystallite size of the calcined in ambient air natural calcites was estimated based on powder XRD studies (Shimadzu 6000 diffractometer using Cu Kα radiation (λ = 1.5418 Å)) and after using the Scherrer formula. The calcite samples used had a grain size lower than 200 mesh. X-ray diffractograms were recorded in the range of 2θ between 10° and 80° with a step of 2°/min.

2.1.2. Elemental chemical analysis (EDX)

The EDXS energy dispersive X-ray spectrometer (INCA x-sight, Oxford Instruments) coupled with a JEOL 2100F transmission electron microscope (TEM) was used for chemical elemental analysis of the calcite materials. A carbon-coated copper grid was employed for depositing the sample for TEM/EDXS measurements. The wt% and at.% compositions of the sample were determined by the provided instrument's software and appropriate calibration procedures.

2.1.3. CO_2 temperature-programmed desorption studies (CO_2-TPDs)

TPD of CO_2 experiments were conducted in a specially designed gas-flow system described elsewhere [17]. The amount of natural calcite material used was 0.5 g, and the flow rate of He used was 30 NmL/min. The fresh sample loaded in the micro-reactor was first calcined in 20%O_2/He at 850 °C for 2 h, purged in He and then cooled quickly to room temperature. The feed was then switched to 2%CO_2/He gas mixture for 30 min. The gas-flow was then switched to He for 15 min until no signal of CO_2 was detected in the mass spectrometer (Balzers, Omnistar). The temperature of the solid was then increased to 800 °C at a heating rate of 30 °C/min to carry out a TPD run. Calibration of the CO_2 signal (m/z = 44) of the mass spectrometer was made based on a standard 1 vol.% CO_2/He gas mixture.

2.2. Catalytic activity studies

The experimental setup used for studying the steam reforming of phenol reaction over the natural calcite materials was described in detail elsewhere [9]. The amount of the calcite sample loaded in the micro-reactor was 0.3 g, and the total flow rate used was 200 NmL/min. The feed reaction mixture used consisted of 0.6%C_6H_5OH/40%H_2O/x%H_2/He (x = 0 and 30 mol%), similar to that encountered at the inlet of a fluidized-bed reactor configuration for wood-biomass gasification [6]. Initially, the catalyst sample loaded in the micro-reactor was calcined in 20%O_2/He gas mixture at 850 °C for 2 h.

The steam reforming of phenol reaction towards hydrogen production over a CaO-containing material can be described by the following network of reactions [7–10,14,15]:

$$C_6H_5OH + 5H_2O \rightarrow 6CO + 8H_2 \qquad (1)$$

$$CO + H_2O \leftrightarrow CO_2 + H_2 \qquad (2)$$

$$CaO + CO_2 \leftrightarrow CaCO_3 \qquad (3)$$

The activity of all calcite materials was studied in the 650–800 °C range. The effect of the presence of H_2 in the feed stream on catalyst activity was also examined.

2.3. In situ DRIFTS studies

In situ DRIFTS chemisorption studies were performed using a PerkinElmer Spectrum GX II FTIR spectrometer equipped with a high-temperature/high pressure controllable DRIFTS cell (Harrick, Praying Mantis) with a gas mixture consisting of 2%CO_2/He (50 NmL/min) or 2%CO_2/40%H_2O/30% or 50%H_2/He (100 NmL/min) at 25 °C and 600 °C, respectively, over a series of five natural calcite materials. About 40 mg of calcite material (pre-calcined *ex situ* at 850 °C in air for 2 h) in fine powder form were placed firmly into the ceramic cup of the DRIFTS cell. Before any spectra were recorded, the sample was pre-treated *in situ* in 20%O_2/Ar at 600 °C for 2 h. Signal averaging was set to 50 scans per spectrum using a 2 cm^{-1} spectra resolution in the 4000–400 cm^{-1} range. The collected DRIFTS spectra were smoothed in order to remove high frequency noise, if necessary, and further analyzed using the software Spectrum (PerkinElmer) for Windows. Deconvolution and curve fitting of the thus derived DRIFTS spectra was performed according to reported guidelines [18] and using Gaussian peak line shapes [19]. The background spectrum of the solid catalyst was taken under Ar flow at the desired reaction temperature. Thus, every DRIFTS spectrum presented here corresponds only to the spectrum of the adsorbed phase after subtracting the spectrum of the solid itself. In the case of recording the spectrum of the solid alone, the background subtracted was that taken with KBr under Ar flow at the same temperature.

CO_2-TPD DRIFTS experiments were performed after 30-min adsorption with 2%CO_2/He at 25 °C. Following adsorption, the DRIFTS cell was purged in Ar flow for 15 min and the temperature was increased to 600 °C in Ar flow. DRIFTS spectra were recorded every 100 °C.

3. Results and discussion

3.1. Catalyst characterization

3.1.1. Conversion of calcites ($CaCO_3$) into calcium oxide

The catalytic activity of the natural calcite materials investigated was due to their active phase of CaO being produced after calcination of the calcite material in 20%O_2/He (50 cm^3/min) at 850 °C for 2 h (0.3 g sample). Fig. 1a presents X-ray diffractograms and Fig. 1b DRIFTS spectra of one of the calcite materials investigated (coded C3), as received ($CaCO_3$) and after calcination at 850 °C. A clear indication about the presence of crystalline CaO

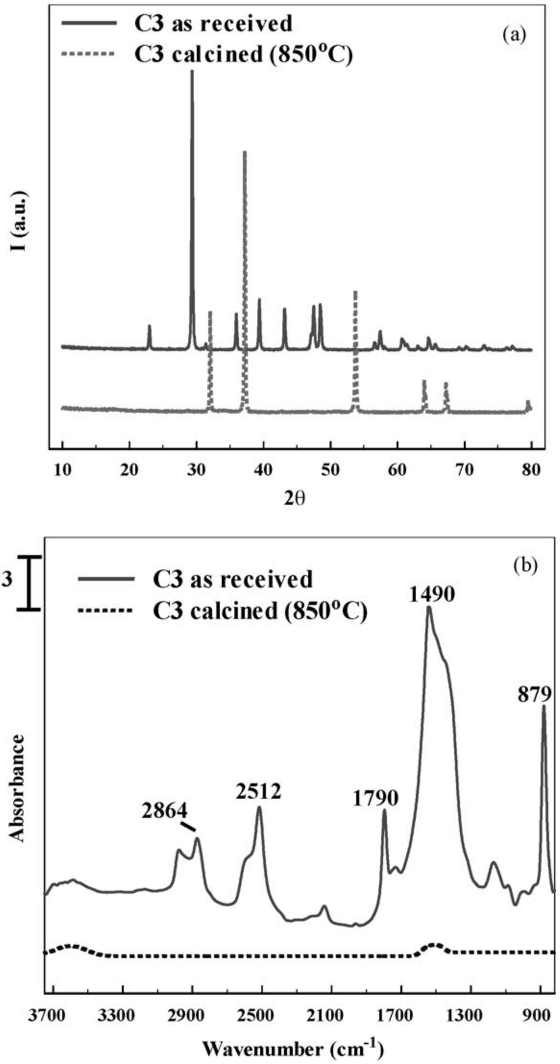

Fig. 1. X-ray diffraction patterns (a) and DRIFTS spectra (b) of C3 natural calcite material as received and after calcination in 20%O_2/He at 850 °C for 2 h (0.3 g sample).

(cubic structure) after calcination is provided in Fig. 1a, where the main 2θ diffraction peaks of calcite-$CaCO_3$ (29.4, 39.4, and 48.54) (JCPDS file 86-174) were absent after calcination, while new strong diffraction peaks (32.04, 37.2, and 53.72) corresponding to CaO were formed (JCPDS file 77-2376). Furthermore, according to the DRIFTS spectra (Fig. 1b), the fundamental infrared bands of calcite material (2864, 2512, and 879 cm^{-1}) [20] and the main infrared bands due to the fundamental vibrational modes of CO_3^{2-} ion (1790, 1490, 1154, and 879 cm^{-1}) [21,22] were absent after calcination. Very similar XRD patterns and DRIFTS spectra were obtained with the other four calcite samples investigated. Only small infrared bands due to surface carbonate (1490 cm^{-1}) and –OH groups were recorded. These were produced due to some exposure of the calcined sample to air during the transfer of the sample to the DRIFTS cell. Pre-treatment of the sample in Ar flow at 600 °C before recording the spectrum at 30 °C did not remove completely the thus formed carbonates.

3.1.2. Specific surface area and XRD measurements

The specific surface area (BET, m^2/g) and the primary mean crystallite size of CaO (d_c, nm) of the five natural calcite materials coded C1–C5 pre-treated at 850 °C in air for 2 h are listed in Table 1.

Table 1
Specific surface area (BET, m^2/g), and mean primary crystal size (d_c, nm) of a series of C1–C5 natural calcite materials after pre-treatment in air at 850 °C for 2 h.

Sample	BET (m^2/g)	d_c (nm)
Calcite C1	9.2	45
Calcite C2	9.4	46
Calcite C3	8.0	51
Calcite C4	8.4	44
Calcite C5	15.6	45

The BET area was found to be in the 8–16 m^2/g range, whereas the mean CaO primary crystal size corresponding to the calcite material C3 was found to be slightly larger (51 nm) than that of the other calcite materials examined (∼45 nm).

3.1.3. Chemical analysis of calcite materials (EDX)

Table 2 presents the wt% composition in metal impurities (Si, Mg, Fe, Al, K, Sn, and Sb) of the C1, C2, and C3 natural calcite materials. In all cases, metal impurities appear less than 0.8 wt% except Si (1.29 wt%, C1), Fe (1.39 wt%, C2), and Sb (1.52 wt%, C3), whereas in terms of at.% composition all metal impurity levels are significantly lower. These results are in harmony with the XRD measurements, where besides CaO no other metal oxide phases due to these metal impurities could be seen. Furthermore, it is important to note here that X-ray photoelectron spectroscopy measurements [23] performed on these samples revealed very low surface concentrations (less than 0.6 at.%) for these metal impurities. Based on the EDX and XPS results, it is strongly suggested that all catalytic performance and CO_2 chemisorption results to be presented next relate to the surface morphological and structural differences of CaO in the samples than to any metal impurity effects. The latter at least should be considered very minor.

3.2. Correlation of catalytic activity with BET (m^2/g) and d_c (nm)

The catalytic steam reforming of phenol (0.6%C_6H_5OH/40%H_2O/30%H_2/He) was investigated at 680 °C over the five pre-calcined natural calcite materials (C1–C5) as described in Section 2.2. Fig. 2a and b compares the specific integral rate of phenol conversion (R_P, μmol $C_6H_5OH/(m^2\ min)$) into CO, CO_2, and H_2 (only small amounts of CH_4 were measured) with the BET surface area (m^2/g) and the primary mean crystal size of CaO (d_c, nm), respectively, for the pre-calcined natural calcite materials, C1–C5. It is observed that the calcite material coded C3 demonstrates the highest specific rate of phenol conversion among all the other calcite materials tested (at least three times higher activity is observed), and that the order of catalytic activity obtained is C3 >> C1 > C2 > C4 > C5.

Fig. 2a also illustrates that there is no correlation between the BET area and the specific catalytic activity measured for the five calcites investigated. According to the EDX and XPS results mentioned in Section 3.1.3, the latter result supports the view that the rate of reaction depends not only on the number density of

Table 2
Concentration (wt%) of metal impurities in the C1, C2, and C3 natural calcite materials.

Metal impurities (wt%)	Calcite C1	Calcite C2	Calcite C3
Si	1.29	0.33	0.09
Mg	0.43	–	0.39
Fe	0.22	1.39	–
Al	0.37	–	–
K	0.06	–	–
Sn	–	–	0.79
Sb	–	–	1.52

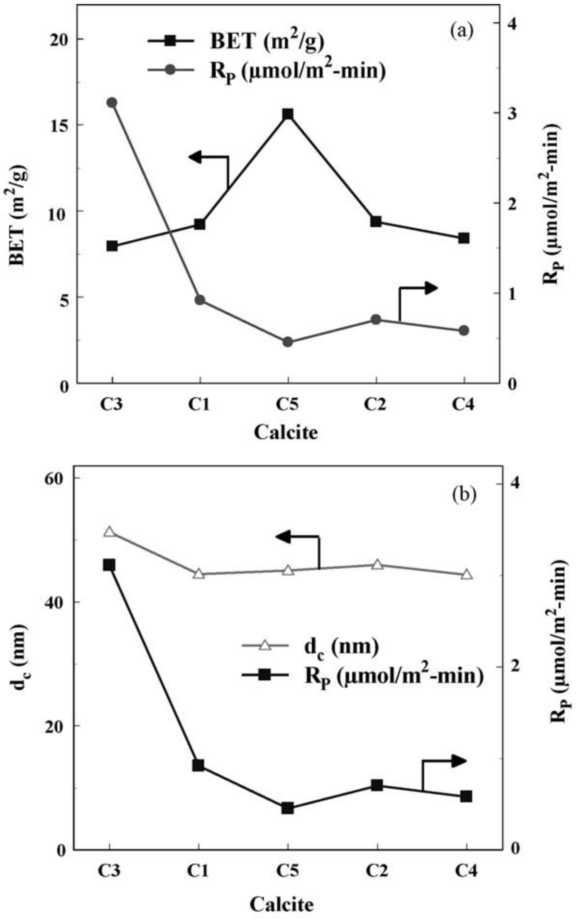

Fig. 2. Correlation of specific rate (µmol/(m^2 min)) of phenol conversion, R_P, with the (a) specific surface area (BET, m^2/g), and (b) mean primary crystal size (d_c, nm) of CaO derived from five natural calcite materials, C1–C5. Feed composition used: 0.6%C_6H_5OH/40%H_2O/30%H_2/He; W_{cat} = 0.3 g; T = 680 °C; F_T = 200 mL/min.

catalytic sites of the CaO surface, but also on the *intrinsic reactivity* of such sites for each CaO surface investigated. The latter is expected to be influenced by the surface morphology and defects present in the primary crystals of the CaO investigated in spite of their similar primary crystal size. Davydov et al. [24] have reported that the structure of an oxide surface provides surface oxygen ions with different effective negative charge and, therefore, a different basic site adsorption strength and reactivity. Based on the results of Fig. 2b it appears that the C3 calcite material after calcination in air at 850 °C resulted in a CaO phase with slightly larger primary crystals than the other four calcite materials but apparently with different surface morphological characteristics that favored phenol steam reforming activity. On the other hand, the CaO surface derived from the C5 calcite material exposed the largest concentration of catalytic sites (based on the BET area, Fig. 2a) but apparently with low site reactivity towards phenol steam reforming, resulting, therefore, in the lowest specific reaction rate (Fig. 2a).

3.3. Catalytic performance of the best calcite material C3

Fig. 3 presents results of the phenol conversion (X_P, %) and the specific integral rate of phenol conversion (R_P, µmol C_6H_5OH/(m^2 min)) obtained in the 650–800 °C range after using the feed composition of 0.6%C_6H_5OH/40%H_2O/He over the C3 calcite material which exhibited the best activity among all the natural calcite materials tested (see Fig. 2). Also, Fig. 3 presents results of the effect of 30 mol% of H_2 in the feed stream on the phenol conversion. It was found that both the conversion and the specific rate of phenol conversion increase with increasing reaction temperature. In the case where H_2 was present in the feed steam, a significant decrease of phenol conversion by more than 50% was observed in the low 650–700 °C temperature range. The latter result is in good agreement with those reported in the literature [25–29]. In particular, Taralas [25] investigated the steam reforming reaction of *n*-heptane using commercial limestone, dolomites, and NiMo/γ-Al_2O_3 catalysts. He observed a decrease in the total conversion of *n*-heptane to H_2 by increasing the amount of hydrogen in the feed stream, where he concluded that addition of hydrogen leads to an increased concentration of cracked hydrocarbon and unsaturated hydrocarbon products. Also, Simell et al. [26] and Aldén et al. [27] studied the steam reforming reaction of benzene and naphthalene, respectively, over calcined dolomite, where they found that hydrogen was dissociatively adsorbed onto the active sites of calcined dolomite (e.g., Mg^{2+}–O^{2-} and Ca^{2+}–O^{2-}) suppressing, therefore, the decomposition of benzene and naphthalene. In addition, Jess [28] and Garcia and Hüttinger [29] have studied the non-catalytic steam reforming and decomposition of benzene, toluene, and naphthalene, respectively, where they showed that the addition of H_2 leads to a decrease in the formation of CO, suggesting that hydrogen is a strong inhibitor of these specific hydrocarbon steam reforming reactions.

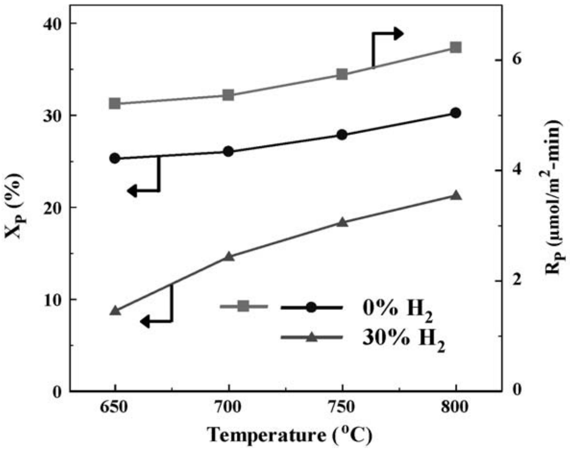

Fig. 3. Dependence of phenol conversion (X_P, %) and specific reaction rate (R_P) on reaction temperature and H_2 concentration in the feed stream for the CaO derived from the natural calcite C3. Feed composition used: 0.6%C_6H_5OH/40%H_2O/x%H_2/He, x = 0 or 30 mol%; W_{cat} = 0.3 g; F_T = 200 mL/min.

All the above results suggest that atomic hydrogen is adsorbed on the O^{n-} anions of the CaO surface, following heterolytic splitting of molecular H_2 onto a Ca^{2+}–O^{2-} ion pair, blocking, therefore, active sites of the CaO that are effective for decomposition/reaction steps of phenol and water (reactions (1) and (2)). The fact that only small concentrations of benzene byproduct were measured in the present phenol steam reforming catalytic work suggest that hydrogenation of phenol into less reactive byproducts towards reforming must be excluded.

3.4. CO_2 chemisorption at 25 °C followed by TPD

Fig. 4 presents TPD response curves of CO_2 obtained under He flow for the C1, C2, and C3 natural calcite materials following calcination at 850 °C (see Section 2.1.3). All TPD-CO_2 profiles start at $T > 500$ °C showing high strength for the basic sites of the CaO surface in agreement with literature [30]. Three well-resolved carbon dioxide desorption peaks are obtained for the pre-calcined

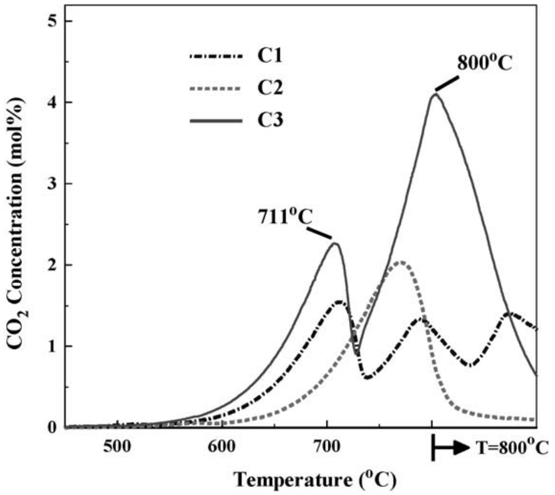

Fig. 4. Temperature-programmed desorption (TPD) response curves of CO_2 under He flow obtained over the CaO derived from the calcite materials C1, C2, and C3. Adsorption conditions: 2%CO_2/He, 25 °C, and 30 min. Desorption conditions: Q_{He} = 30 NmL/min and β = 30 °C/min.

C1 natural calcite material with peak maxima at 715, 790, and 800 °C, the latter obtained under isothermal desorption conditions at 800 °C (see Fig. 4). The latter behavior is discussed in Section 3.5.2. In the case of pre-calcined C2 natural calcite material, only one CO_2 peak centered at 774 °C with a shoulder at the rising part of it was observed, while for the pre-calcined C3 natural calcite material two distinct desorption peaks centered at 711 and 800 °C are obtained with shoulders at the rising part of the first peak and at the falling part of the high-temperature desorption peak.

The above CO_2-TPD results practically imply that at least two kinds of adsorbed carbonate species are formed on the surface of CaO derived from the natural calcite materials investigated in accordance with the *in situ* DRIFTS studies that follow (see Section 3.5). The amount of CO_2 adsorbed on the surface of each natural calcite material (up to 800 °C until no desorption of CO_2 was seen) was found to follow the order: C3 (60.1 μmol/m^2) >> C1 (30 μmol/m^2) > C5 (19.3 μmol/m^2) ≈ C2 (18.0 μmol/m^2) ≈ C4 (18.6 μmol/m^2). It is important to note that this order of CO_2 chemisorption is in very good agreement with the specific activity measurements for steam reforming of phenol over the same series of natural calcite materials (see Fig. 2), and supports the view that the higher the concentration (μmol/m^2) of basic surface sites (oxygen anions) the higher the specific activity (μmol/(m^2 min)) of the calcite towards steam reforming of phenol. It has been reported that the basic sites are essential for the dissociative adsorption of steam that participates in reactions (1) and (2) but also for suppressing carbon deposition occurred during steam reforming of phenol on the surface of CaO [1,2]:

$$C + H_2O \leftrightarrow CO + H_2 \tag{4}$$

Besides the importance of the concentration of basic sites of the CaO for enhancing catalyst activity in the present phenol steam reforming reaction, the strength of CO_2 chemisorption (reaction product) is also very important since the latter competes for the same adsorption sites with the water and phenol (reactant species) towards dissociation steps [8,10]. Thus, it is essential that CaO surface is able during reaction to generate available free active catalytic sites for the adsorption of phenol and water, and in turn to promote the reaction of the derived intermediate species towards CO_2 and H_2 final products.

In the following section *in situ* DRIFTS-CO_2 chemisorption and desorption studies were conducted in order to obtain fundamental information on the *nature of adsorbed carbonate species* formed on the surface of CaO derived from each calcite material, after calcination as reported in Section 2.3, under various gas atmospheres.

3.5. *in situ DRIFTS*

3.5.1. *Adsorbed surface carbonates on CaO derived from C1 and C3 natural calcite materials*

The characterization of adsorbed carbonate species formed after exposing the CaO surface of the two most active natural calcite materials (C1 and C3, Fig. 2) on 2%CO_2/He and 2%CO_2/40%H_2O/30% H_2/He gas mixtures at 25 °C and 600 °C, respectively, were studied by *in situ* DRIFTS (see Section 2.3). It has been reported [31–36] that CO_2 reacts predominantly with O^{2-} and OH^- sites present on a metal oxide surface producing unidentate, bicarbonate, bridging and bidentate carbonate structures. In the case of CaO, *unidentate carbonate* appears to be the main species formed on the surface of CaO-containing materials [35,36].

Fig. 5a shows *in situ* DRIFTS spectra recorded in the 1800–1500 cm^{-1} range over the CaO derived from the C1 natural calcite material (following calcination as reported in Section 2.3) after

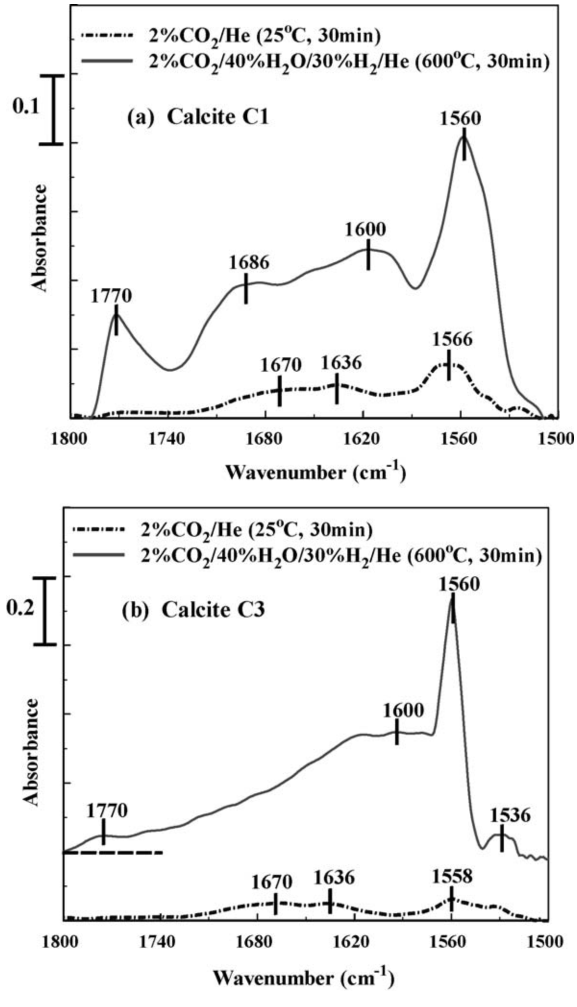

Fig. 5. *In situ* DRIFTS spectra recorded in the 1800–1500 cm^{-1} range after 30 min of 2%CO_2/He and 2%CO_2/40%H_2O/30%H_2/He gas treatment at 25 °C and 600 °C, respectively, over CaO derived from (a) C1 and (b) C3 natural calcite materials following calcination as described in Section 2.3.

30 min exposure to a $2\%CO_2/He$ or $2\%CO_2/40\%H_2O/30\%H_2/He$ gas mixture at 25 °C and 600 °C, respectively. In the case of CO_2 chemisorption at 25 °C (lower spectrum), the two overlapping broad IR bands recorded at 1670 and 1636 cm^{-1} are assigned to the OCO_{as} vibrational mode of two different bicarbonate species, whereas the IR band recorded at 1566 cm^{-1} with a shoulder to the lower wave number side is attributed to different unidentate carbonate species (OCO_{as} stretching vibration mode) coordinated to the calcium ions [32,34–36]. The infrared spectrum of CO_2/CaO system presented in Fig. 5a (lower spectrum) is in harmony with that reported by Zaki et al. [34] and Philipp and Fujimoto [36] who reported that *unidentate carbonate* is the dominant adsorption state. It should be noted that the relative abundance of the various CO_2 adsorption states depends on the CO_2 partial pressure and temperature of adsorption.

In the case of exposing the CaO derived from the C1 calcite to the $2\%CO_2/40\%H_2O/30\%H_2/He$ gas mixture for 30 min at 600 °C (upper spectrum, Fig. 5a), the infrared bands (1670, 1636, and 1566 cm^{-1}) due to unidentate and bicarbonate species observed at 25 °C after $2\%CO_2/He$ gas treatment were significantly increased, particularly the IR band corresponding to the *unidentate carbonate*, and slightly shifted, whereas a new infrared band (1770 cm^{-1}) assigned to the C=O stretching vibrational mode of *bridged carbonate* [35,36] was developed. The very broad IR band recorded at 1600 cm^{-1} also contains the OCO_{as} vibrational mode of formate species [35], while that at 1636 cm^{-1} of adsorbed molecular water (bending mode), if the latter is present at 600 °C. Adsorbed formate species was clearly identified based on the νCH band developed in the 2930–2950 cm^{-1} range (not shown here) for the C1, C2, and C3 calcites investigated.

In situ DRIFTS spectra were also recorded over the CaO derived from the C3 natural calcite material (Fig. 5b) using the same gas mixtures of $2\%CO_2/He$ and $2\%CO_2/40\%H_2O/30\%H_2/He$ at 25 °C and 600 °C, respectively, after 30 min of treatment. A very similar infrared spectrum after CO_2 chemisorption at 25 °C was performed was obtained (lower spectrum, Fig. 5b) as with the C1 natural calcite material (lower spectrum, Fig. 5a). However, in the presence of $2\%CO_2/40\%H_2O/30\%H_2/He$ gas mixture at 600 °C the spectrum is different with large changes in the relative population of the various adsorbed CO_2 structures (compare upper spectra in Fig. 5a and b). A significant increase in the surface concentration of unidentate and bicarbonate species was observed, while a lower concentration of bridged carbonate species appears as compared to calcite C1. The results of Fig. 5 indicate that the chemical structure of the various carbonate species formed on both CaO surfaces derived from C1 and C3 calcite materials are the same, and the only difference being the relative population of these species (Fig. 5a and b).

3.5.2. Comparison of carbonate species formed in the CaO derived from C1, C2, and C3 calcites

In situ DRIFTS spectra (in Kubelka–Munk (K–M) units) recorded in the 1800–1500 cm^{-1} range after 5 min of CO_2 chemisorption at 25 °C (2% CO_2/He) over the CaO surfaces derived from the C1, C2, and C3 natural calcite materials are presented in Fig. 6a. Deconvolution and curve fitting of the spectrum corresponding to C3 as described in Section 2.3 is shown in Fig. 6a (lower spectrum). According to Fig. 6a, the most intense IR bands observed are two different kinds of bicarbonate (1680 and 1636 cm^{-1}) and unidentate carbonate (1560 and 1536 cm^{-1}) species. A small IR band due to bridged carbonate (1770 cm^{-1}) is clearly seen in the case of C1 calcite material. The kinds of carbonate species identified were all formed after the first 5 min of exposure of the CaO to the $2\%CO_2/He$ gas mixture, where only very small increases in the IR band intensities were observed after 30 min of exposure.

Comparison of the integral band area of the various carbonate bands obtained after deconvolution and curve fitting (e.g., lower spectrum in Fig. 6a) of the DRIFTS spectra shown in Fig. 6a is illustrated in Fig. 7. The integral band area of unidentate carbonate species is considered the sum of the bands centered at 1560 and 1536 cm^{-1}, while that of bicarbonate species the sum of the bands centered at 1680 and 1636 cm^{-1}. It is shown that the surface concentration of the unidentate carbonate is larger for C2 compared to C1 and C3 natural calcite materials. Fig. 7 also shows that the integral band area of the bicarbonate species is larger for C1 compared to C2 and C3, whereas no significant differences were observed for the bridged carbonate species. The above results support the view that the higher the surface concentration of unidentate carbonate species (Figs. 6a and 7) the lower the activity of the CaO derived from the natural calcite material investigated (Fig. 2). The latter is true assuming that no significant variation in the extinction coefficient for the three kinds of adsorbed carbonate molecular structures exists.

After a 30-min of $2\%CO_2/He$ gas treatment (Section 2.3) it was found that at 600 °C the integral area of IR band due to unidentate carbonate (1560 cm^{-1}) was slightly decreased, whereas that due to bicarbonate species was significantly decreased. This result is related to the relative thermal stability of the two kinds of

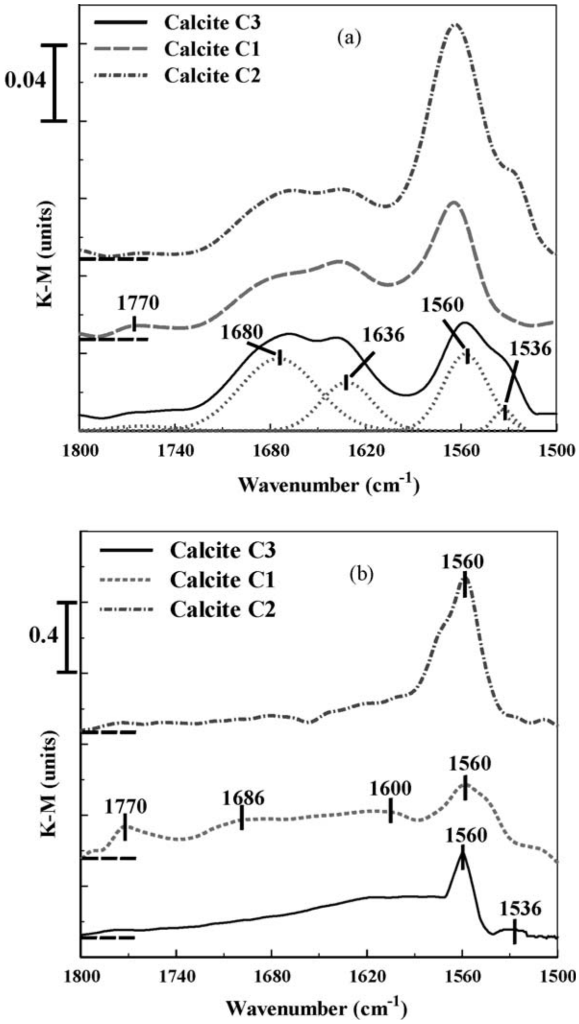

Fig. 6. *In situ* DRIFTS spectra (in Kubelka–Munk (K–M) units) recorded in the 1800–1500 cm^{-1} range after (a) 5 min of CO_2 chemisorption with $2\%CO_2/He$ gas mixture at 25 °C, and (b) 30 min gas treatment in $2\%CO_2/40\%\ H_2O/30\%H_2/He$ at 600 °C over CaO derived from C1, C2, and C3 calcite materials.

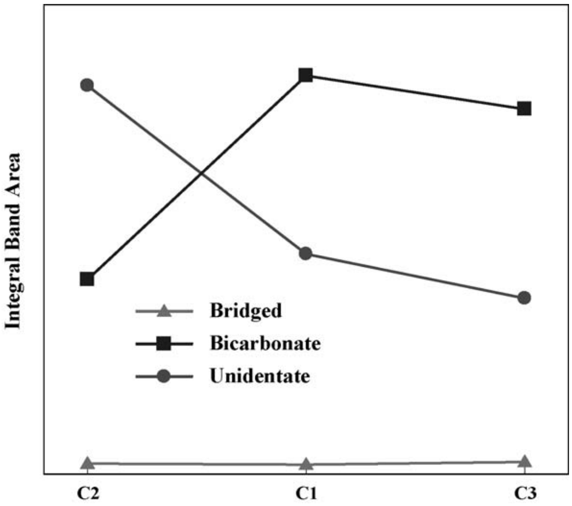

Fig. 7. Integral band area corresponding to the three most important adsorbed carbonate species formed on the surface of CaO, the latter derived following calcination of the natural calcite materials C1, C2, and C3 as described in Section 2.3, followed by CO_2 chemisorption at 25 °C.

carbonate species, and it is in harmony with other experimental observations reported according to CO_2-TPD [23] and FTIR studies [32,33,36].

The presence of unidentate and bidentate carbonates at high temperatures ($T > 600$ °C) over CaO during TPD studies has been reported [36]. The authors have proposed that this could be the result of the partial transformation of unidentate into bidentate carbonate species because of the lowering of the basic strength of surface oxygen due to dehydration. In the CO_2-TPD trace of Fig. 4 for the CaO derived from the C1 calcite material, two thermal desorption peaks were found in the 720–800 °C range. This could be the result of the transformation of some unidentate into bidentate carbonate species, the latter reported to be more thermally stable [37].

Fig. 6b presents DRIFTS spectra recorded in the 1800–1500 cm^{-1} range for CaO surfaces derived after calcination (see Section 2.3) of C1, C2, and C3 natural calcite materials, after 30 min of gas treatment in $2\%CO_2/40\%H_2O/30\%H_2/He$ gas mixture at 600 °C. It is clearly illustrated that in the presence of water and hydrogen the surface concentration of all adsorbed carbonate species detected (bridged, bicarbonate, and unidentate) increases (compare K–M unit intensity in Fig. 6a and b), whereas the concentration of unidentate carbonate species with higher thermal stability than the bicarbonate species was substantial.

After increasing the H_2 concentration in the feed stream from 30 to 50 vol.% the surface concentration of bicarbonates and –OH species formed was largely reduced, while that of unidentate carbonate was practically remained constant. Detailed mechanistic scheme and explanations for this behavior (H_2 inhibiting effect of steam reforming activity, see Fig. 2) will be reported elsewhere [23].

The present catalytic activity and *in situ* DRIFTS-CO_2 chemisorption results (Figs. 2, 6 and 7) support the view that the lower the specific activity of the CaO surface derived from the natural calcite material (after calcination as reported in Sections 2.2 and 2.3) the higher the surface concentration of unidentate carbonates (broad IR band at 1560 cm^{-1}) formed. The CaO surface derived from the calcite material C3 which demonstrated the best specific catalytic activity (Fig. 2) exhibits the lowest surface concentration of unidentate carbonates and, therefore, exposes a larger concentration of free active sites for the decomposition/reaction of phenol and water. In addition, based on the bonding mode of unidentate carbonate, and the fact that dissociation of water requires a pair site of adjacent Ca^{2+}–O^{2-} ions, it is apparent the inhibiting role of CO_2 during steam reforming of phenol over CaO surfaces.

4. Conclusions

The following conclusions can be derived from the results of the present work:

(a) The higher specific catalytic activity towards the steam reforming of phenol reaction observed over the CaO surface derived from the natural calcite material C3 compared to all other calcites tested ($C3 >> C1 > C2 > C4 > C5$) seems to correlate with the higher site reactivity (e.g., different surface morphology and defect sites) and also to the largest concentration ($\mu mol/m^2$) of basic sites (TPD-CO_2 studies) and the least concentration ($\mu mol/g$) of unidentate carbonate species formed.

(b) The presence of hydrogen in the feed stream (30–50 vol.%) of the phenol steam reforming reaction ($0.6\%C_6H_5OH/40\%H_2O/He$) leads to a significant reduction in phenol conversion in the 650–800 °C range suggesting that final accommodation of hydrogen (H) on the O^{2-} sites, following a heterolytic H_2 dissociation step onto a Ca^{2+}–O^{2-} site pair, blocks active sites for the decomposition/reaction of phenol and water reactant molecules.

(c) *In situ* DRIFTS-CO_2 chemisorption studies from a gas mixture $2\%CO_2/40\%H_2O/30\%H_2/He$ at 600 °C demonstrated the existence of bridged, bicarbonate, and unidentate carbonates as main CO_2 chemisorbed species, with the latter being mainly the predominant one, lowering, therefore, the activity of the CaO surface. A substantial decrease in the surface concentration of bicarbonate and –OH species was observed when adsorption of CO_2 took place from a gas mixture containing H_2 ($2\%CO_2/40\%H_2O/x\%H_2/He$) after the concentration of the latter was increased from 30 to 50 vol.%. The latter probes the inhibiting role of H_2 during steam reforming of phenol over the present CaO surfaces.

Acknowledgements

The financial support of the European Union (Project No. 5183309 (SES6), 6th FP) is gratefully acknowledged. The authors express their sincere thanks to the group of Professor J.L.G. Fierro (ICP/CSIC Madrid, Spain) for the TEM/EDX and XPS measurements.

References

[1] J.N. Armor, Appl. Catal. A: Gen. 176 (1999) 159.
[2] M.A. Peña, J.P. Gómez, J.L.G. Fierro, Appl. Catal. A: Gen. 144 (1996) 7.
[3] D. Dayton, A Review of the Literature on the Catalytic Biomass Tar Destruction, NREL/TP-510-32815, National Renewable Energy Laboratory, 2002.
[4] T.A. Milne, N. Abatzoglou, R.J. Evans, Biomass Gasifier Tars: Their Nature, Formation and Conversion, NREL/TP-570-25357, National Renewable Energy Laboratory, USA, 1989.
[5] R. Zhang, R.C. Brown, A. Suby, K. Cummer, Energy Conv. Manage. 45 (2004) 995.
[6] European Project, 6th FP, No. 5183309 (SES6), Biomass Fluidized Bed Gasification with In-Situ Hot Gas Cleaning, 2006.
[7] D. Wang, S. Czernik, D. Montané, M. Mann, E. Chornet, Ind. Eng. Chem. Res. 36 (1997) 1507.
[8] K. Polychronopoulou, J.L.G. Fierro, A.M. Efstathiou, J. Catal. 228 (2004) 417.
[9] K. Polychronopoulou, C.N. Costa, A.M. Efstathiou, Appl. Catal. A: Gen. 272 (2004) 37.
[10] K. Polychronopoulou, A. Bakandritsos, V. Tzitzios, J.L.G. Fierro, A.M. Efstathiou, J. Catal. 241 (2006) 132.
[11] J. Delgado, M.-P. Aznar, J. Corella, Ind. Eng. Chem. Res. 35 (1996) 3637.
[12] J. Delgado, M.-P. Aznar, J. Corella, Ind. Eng. Chem. Res. 36 (1997) 1535.
[13] S. Rapagná, N. Jand, A. Kiennemann, P.U. Foscolo, Biomass Bioenergy 19 (2000) 187.

[14] M.R. Mahishi, D.Y. Goswami, Int. J. Hydrogen Energy 32 (2007) 2803.
[15] B. Balasubramanian, A.L. Ortiz, S. Kaytakoglu, D.P. Harrison, Chem. Eng. Sci. 54 (1999) 3543.
[16] C. Pfeifer, B. Puchner, H. Hofbauer, Int. J. Chem. Rec. Eng. 5 (2007) A9.
[17] C.N. Costa, T. Anastasiadou, A.M. Efstathiou, J. Catal. 194 (2000) 250.
[18] B.C. Smith, Fundamentals of Fourier Transform Infrared Spectroscopy, CRC Press, 1996.
[19] F.M. Hoffmann, Surf. Sci. Rep. 3 (1983) 107.
[20] C. Breen, F. Clegg, M.M. Herron, G.P. Hild, S. Hiller, T.L. Hughes, T.G.L. Jones, A. Matteson, J. Yarwood, J. Petrol. Sci. Eng. 60 (2008) 1.
[21] C.H. Linga, K.V. Raju, N. Narasimhulu, O. Gopal, J.L. Rao, B.C.V. Reddy, Spectrochim. Acta Part A 59 (2003) 2955.
[22] K.V. Narasimhulu, J.L. Rao, Spectrochim. Acta Part A 56 (2000) 1345.
[23] D.A. Constantinou, J.L.G. Fierro, A.M. Efstathiou, J. Catal. (submitted).
[24] A.A. Davydov, M.L. Shepotko, A.A. Budneva, Catal. Today 24 (1995) 225.
[25] G. Taralas, Ind. Eng. Chem. Res. 35 (1996) 2121.
[26] P.A. Simell, E.K. Hirvensalo, V. Smolander, A.O.I. Krause, Ind. Eng. Chem. Res. 38 (1999) 1250.
[27] H. Aldén, E. Björkman, M. Carlsson, A. Waldheim, in: Proceedings of the Conference on Advances in Thermochemical Biomass Conversion, Blackie Academic & Professional, London, (1994), p. 216.
[28] A. Jess, Fuel 75 (12) (1996) 1441.
[29] X.A. Garcia, K.J. Hüttinger, Fuel 68 (1989) 1300.
[30] G. Zhang, H. Hattori, K. Tanabe, Appl. Catal. 36 (1988) 189.
[31] P. Käβner, M. Baerns, Appl. Catal. A: Gen. 139 (1996) 107.
[32] R. Philipp, K. Omata, A. Aoki, K. Fujimoto, J. Catal. 134 (1992) 422.
[33] Y. Xu, L. Yu, C. Cai, J. Huang, X. Guo, Catal. Lett. 35 (1995) 215.
[34] M.I. Zaki, H. Knözinger, B. Tesche, G.A.H. Mekhemer, J. Colloid Interf. Sci. 303 (2006) 9.
[35] G. Busca, V. Lorenzelli, Mater. Chem. 7 (1982) 89.
[36] R. Philipp, K. Fujimoto, J. Phys. Chem. 96 (1992) 9035.
[37] N. Alarcón, X. García, M. Centeno, P. Ruiz, A. Gordon, Surf. Interf. Anal. 31 (2001) 1031.